JPn Neuroscience
The Journal of Physiology

J Physiol 593.19 (2015) pp 4485–4498

Contrast invariance of orientation tuning in cat primary visual cortex neurons depends on stimulus size

Yong-Jun Liu, Maziar Hashemi-Nezhad and David C. Lyon

Department of Anatomy and Neurobiology, School of Medicine, University of California, 364 Med Surge II, Irvine, CA 92697, USA

Key points

- The process of orientation tuning is an important and well-characterized feature of neurons in primary visual cortex.
- The combination of ascending and descending circuits involved is not only relevant to understanding visual processing but the function of neocortex in general.
- The classic feed-forward model of orientation tuning predicts a broadening effect due to increasing contrast; yet, experimental results consistently report contrast invariance.
- We show here that contrast invariance actually depends on stimulus size such that large stimuli extending beyond the neuron's receptive field engage circuits that promote invariance, whereas optimally sized, smaller stimuli result in contrast variance that is more in line with the classical orientation tuning model.
- These results illustrate the importance of optimizing stimulus parameters to best reflect the sensory pathways under study and provide new clues about different circuits that may be involved in variant and invariant response properties.

Abstract Selective response to stimulus orientation is a key feature of neurons in primary visual cortex, yet the underlying mechanisms generating orientation tuning are not fully understood. The combination of feed-forward and cortical mechanisms involved is not only relevant to understanding visual processing but the function of neocortex in general. The classic feed-forward model predicts that orientation tuning should broaden considerably with increasing contrast; however, experimental results consistently report contrast invariance. We show here, in primary visual cortex of anaesthetized cats under neuromuscular blockade, that contrast invariance occurs when visual stimuli are large enough to include the extraclassical surround (ECS), which is likely to involve circuits of suppression that may not be entirely feed-forward in origin. On the other hand, when stimulus size is optimized to the classical receptive field of each neuron, the population average shows a statistically significant 40% increase in tuning width at high contrast, demonstrating that contrast variance of orientation tuning can occur. Conversely, our results also suggest that the phenomenon of contrast invariance relies in part on the presence of the ECS. Moreover, these results illustrate the importance of optimizing stimulus parameters to best reflect the neural pathways under study.

(Resubmitted 23 June 2015; accepted after revision 27 July 2015; first published online 31 July 2015)
Corresponding author D. C. Lyon: Department of Anatomy and Neurobiology, School of Medicine, 364 Med Surge II, University of California, Irvine, CA 92697-1275, USA. Email: dclyon@uci.edu

Abbreviations CRF, classical receptive field; CV, circular variance; ECS, extraclassical receptive field; HWHH, half-width at half-height; LGN, lateral geniculate nucleus; V1, primary visual cortex.

Y.-J. Liu and M. Hashemi-Nezhad contributed equally to this work.

DOI: 10.1113/JP271180

Introduction

Orientation tuning is an emergent property of neurons in the primary visual cortex (V1) (Hubel & Wiesel, 1962). Despite extensive progress in the field, the underlying mechanisms generating orientation tuning are still debated (Reid & Alonso, 1996; Sompolinsky & Shapley, 1997; Ferster & Miller, 2000; Alitto & Dan, 2010). The classic feed-forward model by Hubel & Wiesel (1962) predicts that orientation tuning should broaden with increasing contrast (see Rose & Blakemore, 1974; Troyer *et al.* 1998; Carandini, 2007). However, several subsequent reports found that orientation tuning is invariant to changes in contrast (Sclar & Freeman, 1982; Skottun *et al.* 1987; Anderson *et al.* 2000; Alitto & Usrey, 2004). As a result, many modelling studies have since attempted to explain the emergence of orientation tuning using this constraint with a balanced cortical inhibition, or other forms of response amplitude reduction such as synaptic noise (Ferster, 1988; Carandini & Heeger, 1994; Sompolinsky & Shapley, 1997; Hirsch *et al.* 1998; Troyer *et al.* 1998; Somers *et al.* 2002; Palmer & Miller, 2007; Stimberg *et al.* 2009; Tan *et al.* 2011; Sadagopan & Ferster, 2012).

However, most studies demonstrating contrast invariance of orientation tuning (see above) have used relatively large visual stimuli that are likely to have extended beyond the cell's classical receptive field (CRF) and into the extraclassical surround (ECS). Importantly, inclusion of the ECS can significantly reduce response amplitude (DeAngelis *et al.* 1994; Sengpiel *et al.* 1997; Walker *et al.* 2000; Akasaki *et al.* 2002; Cavanaugh *et al.* 2002*b*; Liu *et al.* 2011) and sharpen orientation tuning of V1 cells (Henry *et al.* 1974; Chen *et al.* 2005; Xing *et al.* 2005). This reduction in amplitude and sharpening of orientation tuning has been shown to result through a subtractive suppression (Okamoto *et al.* 2009) that may not be entirely feed-forward in origin (Angelucci & Sainsbury, 2006; Hashemi-Nezhad & Lyon, 2012; Liu *et al.* 2013*b*). In order to establish whether stimulus size plays a role in the contrast invariance of orientation tuning, we determined, in V1 of anaesthetized cats under neuromuscular blockade, the CRF size of each neuron at low and high contrast, and compared the orientation tuning profiles to those derived from large-field stimuli, CRF + ECS. Inclusion of the ECS yields results consistent with earlier work in that orientation tuning is invariant to a large increase in contrast. However, without the ECS, we find orientation tuning is significantly broader at high contrast compared to low contrast. These results demonstrate that orientation tuning of the CRF is not invariant to contrast in a manner somewhat consistent with the classic feed-forward excitatory model. Conversely, contrast invariance resulting from the ECS indicates that recruitment of circuits involving integration of a large representation of visual space, such as feedback from higher visual cortex (Angelucci *et al.* 2002; Cantone *et al.* 2005) or di-synaptic horizontal connections (Gilbert & Wiesel, 1989; Liu *et al.* 2014), probably plays a key role in this phenomenon. Furthermore, these results are an important reminder that in order to fully understand the mechanisms underlying the emergence of orientation tuning in V1 it is necessary to consider optimal and large-field stimuli separately, as well as the interaction between them.

Methods

Ethical approval

All procedures complied with the guidelines of the Institutional Animal Care and Use Committee of the University of California, Irvine.

Animal preparation

Experiments were carried out *in vivo* on 12 adult cats between 8 and 24 months of age of either sex weighing 2.4–5 kg. Animals were initially anaesthetized with a mixture of ketamine (21 mg kg^{-1}, I.M.) and xylazine (3 mg kg^{-1}, I.M.), and then tracheal and venous cannulations were performed. Anaesthesia was maintained by inhalation of isoflurane (0.2–1.0%) in a 2:1 mixture of nitrous oxide and oxygen. In order to ensure a proper level of anaesthesia throughout the experiment, lung pressure, ECG and EEG were monitored. In addition, CO_2 was maintained between 4.0 and 4.5% and body temperature was kept near 37°C through a homeothermic monitor and heating pad (Harvard Apparatus, Holliston, MA, USA). Pupils were dilated and accommodation blocked with atropine sulfate (1%). Air-permeable corrective contact lenses were used to protect the corneas. A craniotomy was made above the dorsal surface of area 17 (V1) and the dura was removed. For visual recording, eye movements were prevented by inducing neuromuscular blockade with a bolus of vecuronium bromide (0.6 mg in 1 ml, I.V.) and maintained throughout the experiment with 2.0 mg kg^{-1} every hour in a solution of 5% dextrose and lactated Ringer solution containing dexamethasone (0.5 mg kg^{-1} h^{-1}, I.V.).

Electrophysiology and visual stimulation

Single unit extracellular recordings were made using epoxy insulated tungsten microelectrodes (3–7 MΩ; FHC, Bowdoin, ME, USA). Electrodes were placed perpendicular to the surface at 3–4 mm from the midline in order to estimate superficial (<600 μm), middle (600–1200 μm) and infragranular (>1200 μm)

layers by cortical depth as described previously elsewhere (Schummers *et al.* 2007; Hashemi-Nezhad & Lyon, 2012). Once an electrode was inserted below the cortical surface, the brain was covered by a 1.5% agar solution in saline and then sealed with physiological wax to reduce brain pulsation. Action potentials of isolated neurons were amplified using an Xcell-3 four-channel amplifier (FHC). Evoked action potentials were detected with an online window discriminator and stored digitally using EXPO signal-processing software (courtesy of Dr Peter Lennie and Rob Dobson). The amplified signals were also broadcast over a loudspeaker for subjective analysis.

Visual stimuli were displayed on a 21 inch View Sonic Graphics Series G225f CRT screen (γ calibrated) with a mean luminance of 50 cd m^{-2}. The monitor refreshed at 100 Hz with a resolution of 640 × 480 pixels. Gas-permeable corrective lenses were used to focus the retina on a tangent screen 37 cm away, and artificial pupils of 3 mm in diameter were placed in front of the eyes. The location of the optic disc and the area centralis for each eye were plotted daily with a fibre-optic light source. Stimuli were generated using EXPO software run on a G5 Mac with an ATI Radeon 9200 graphics card. Each cell was stimulated through the dominant eye with the non-dominant eye occluded.

Once a cell was isolated, the approximate location of its receptive field centre and an estimate of the preferred orientation were found by using a circular square-wave grating patch ∼4 deg in diameter. Using the preferred orientation, the diameter of the patch was then decreased to as small as 1 deg to pinpoint the receptive field's centre by moving the stimulus systematically under mouse control, similar to methods described elsewhere (Sceniak *et al.* 2006; Liu *et al.* 2011; Hashemi-Nezhad & Lyon, 2012). Spatial eccentricities of all receptive fields in our experiment were constrained between 2 deg into the upper visual quadrant and 16 deg into the lower quadrant.

Once the receptive field centre of each cell was identified, several visual response properties of the cell were tested in detail in order to identify optimal stimulus parameters. First, the preferred orientation was reassessed more systematically by using orientations sampled every 22.5 deg and a drifting sine-wave grating presented within a circular aperture ∼10 deg in diameter using 100% contrast, a spatial frequency of 0.2 cycles deg^{-1}, and a temporal frequency of 4 Hz. Next, using the preferred orientation and the parameters listed above, the optimal spatial and temporal frequencies were determined. Finally, using all of the obtained optimal parameters (orientation, spatial frequency, temporal frequency) at 100% contrast we tested each neuron's response to different apertures ranging from 0.2 to 30 deg, in 18 steps (see Fig. 1*B*). From the aperture tuning curve, the classical receptive field (CRF) was defined as the aperture size resulting in the greatest mean response (optimal grating), and the

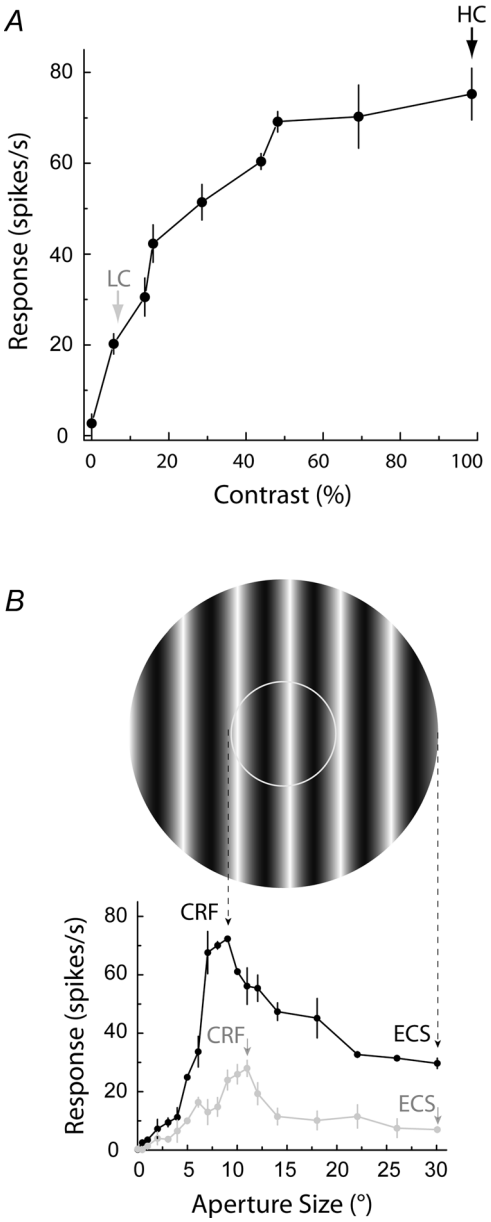

Figure 1. Identification of the classical receptive field (CRF) and extraclassical surround (ECS) at high and low contrast
A, for this example neuron, 100% contrast elicits the maximum response (black arrow) and is chosen as the high contrast (HC). The percentage contrast eliciting 30% of the maximum response is 8% (grey arrow) and is chosen as the low contrast (LC). *B*, the aperture tuning curves for the same neuron at high (black trace) and low (grey trace) contrast are shown. The grating stimulus shown above corresponds to the high contrast CRF (inner white circle) and the high contrast ECS (outer edge of the whole aperture), with dashed arrows pointing to the corresponding peak response at 9 deg and the point of subsequent maximum suppression at 30 deg. The representative low contrast grating stimulus is not shown, but the CRF size is slightly larger, 11 deg (left grey arrowhead), as indicated by the rightward shift of the peak response of the grey tuning curve. The low contrast ECS is 30 deg (right grey arrowhead), since this is the point of maximum suppression following the peak.

extraclassical surround (ECS) was defined as the size subsequently leading to the greatest reduction in response, or maximum suppression (Fig. 1*B*).

Following determination of the CRF and ECS at 100% contrast, contrast tuning profiles were obtained using the optimal aperture size (CRF), orientation, and spatial and temporal frequencies, for nine contrasts ranging from 0 to 100% (see example in Fig. 1*A*). If the contrast profile saturated before 100% contrast, the non-saturating contrast was defined as the high contrast and the aperture tuning protocol described above was repeated again to obtain the CRF and ECS at the non-saturating high contrast. Low contrast was defined as 30% of the maximum response (Fig. 1*A*). Low contrast values ranged from 5 to 16% contrast for our cell population. The sizes of CRF and ECS were then determined at this low contrast (see grey trace in Fig. 1*B*). As indicated in Fig. 1*B*, the CRF size at low contrast was larger than the CRF size at high contrast. This was found for a majority of the cells tested (see Results) and is similar to results reported by others (Sceniak *et al.* 1999; Cavanaugh *et al.* 2002*b*; Tailby *et al.* 2007; Hashemi-Nezhad & Lyon, 2012).

Finally, orientation tuning profiles were obtained under optimal spatial and temporal frequencies with CRF and CRF + ECS stimuli shown at high and low contrast. Stimulus sets for each of the four conditions were shown separately, and in different orders for different cells. The visual stimuli were drifting sinusoidal gratings, enveloped by sharp edged circular apertures, and presented on a grey background of the same mean luminance as the stimuli. Stimuli were presented for 2 s, and were repeated four to six times. Each stimulus-set used an inter-stimulus time interval of 2 s and a blank stimulus was used to determine the spontaneous activity.

Data analysis

Number of cells and simple/complex cell classification. For 154 neurons the orientation tuning profiles were obtained for as many as four conditions: high contrast CRF, low contrast CRF, high contrast CRF + ECS, and low contrast CRF + ECS (see examples in Figs 2 and 3). The mean firing rate (F_0) and first harmonic of the Fourier transform (F_1) of the accumulated response were computed. V1 neurons were classified as simple or complex by comparing the F_1/F_0 ratio in response to drifting grating stimuli of optimal spatial frequency and high contrast (Skottun *et al.* 1991). Overall, 27% of neurons were determined to be simple cells ($n = 42/154$). Responses for simple cells were plotted using the first harmonic, whereas mean spike rate was used for complex cells. All four conditions (CRF at high and low contrast; CRF + ECS at high and low contrast) were not completed for all 154 neurons; because of this the numbers of neurons analysed ranged from 105 to 135 depending on the conditions being compared (see Results for details).

Orientation tuning width. The orientation responses were fitted to Gaussian distributions (Carandini & Ferster, 2000; Alitto & Usrey, 2004) using:

$$R_{O_s} = \text{baseline} + R_p e^{-(O_s-O_p)^2/(2\sigma^2)} + R_n e^{-(O_s-O_p+180)^2/(2\sigma^2)} \quad (1)$$

where O_s is the stimulus orientation, R_{O_s} is the response to different orientations, O_p is the preferred orientation, R_p and R_n are the responses at the preferred and non-preferred direction, σ is the tuning width, and 'baseline' is the DC-offset of the Gaussian distribution. Gaussian fits were estimated without subtracting spontaneous activity, similar to the procedures of Alitto & Usrey (2004).

The orientation tuning bandwidth of each tuning curve was measured in degrees as the half-width at half-height (HWHH), which equals $1.18 \times \sigma$ based on the equation above. Note, that our orientation tuning curves typically had two peaks, one for each direction over 360 deg (see Fig. 2*A–L*). For each cell, we chose the higher of the two peaks under the CRF high contrast condition as preferred orientation, which was always the condition yielding the maximum response, and compared the HWHH of this peak across conditions (see Fig. 2*A–D*).

The coefficient of determination (R^2) was used to evaluate the goodness of our fits.

$$R^2 = \left(1 - \sum_{j=1}^{N} (R_n - F_n)^2 / \sum_{j=1}^{N} (R_n - R_0)^2\right) \quad (2)$$

where R_n is the response to the jth stimulus, F_n is the predicted value, and R_0 is the mean response of the actual data (Freeman *et al.* 2002). Files with fits below an R^2 of 0.50 were excluded from further analysis. For each of the four stimulus conditions, high contrast CRF, low contrast CRF, high contrast CRF + ECS, and low contrast CRF + ECS, the mean R^2 and standard deviations were 0.88 ± 0.11, 0.86 ± 0.13, 0.89 ± 0.10, and 0.86 ± 0.12, respectively (see Results for more details).

Circular variance. In addition to HWHH, orientation selectivity was measured by circular variance (CV), a more global measure of the tuning curve (Ringach *et al.* 2002), which was calculated using:

$$\text{CV} = 1 - \sum_n R_n \exp(i2\theta_n) \quad (3)$$

where the angle θ_n is the orientation of the nth stimulus in radians, and R_n is the mean firing rate at orientation θ. For these calculations the spontaneous activity was removed. CV values approaching 0 indicate higher selectivity.

Significance tests. Prior to statistical analysis of groups, we tested whether or not distributions were normal using the Lilliefors test. The distribution of HWHH values was not normal, therefore a Mann–Whitney *U* test was used when making these comparisons. On the other hand, the distributions of CV values were not statistically different from normal; therefore *t* tests were used for comparisons. The distributions of CRF and ECS sizes calculated at high and low contrast were also normal and therefore *t* tests were used for comparisons.

Results

To determine whether stimulus size plays a role in contrast invariance of orientation tuning in V1, we measured detailed orientation responses under each of four stimulus conditions (low contrast CRF, high contrast CRF, low contrast CRF + ECS, and high contrast CRF + ECS) and fitted each tuning curve using a Gaussian model (eqn (1)). Examples for two complex cells (left columns) and two simple cells (right columns) are illustrated in Fig. 2. When contrast is increased for large-field stimulation (CRF + ECS) orientation tuning curves show little to no change in width (Fig. 2, rows 3 and 4). However, tuning width broadens when contrast is increased for the CRF stimulus (Fig. 2, rows 1 and 2). For example, the HWHH of the neuron in the left column increases by 44%, from 25.1 deg (Fig. 2*A*) to 36.1 deg (Fig. 2*B*) when contrast is increased for CRF stimulation, but with the inclusion of the ECS there is little difference in HWHH at low (23.7 deg) and high (22.3 deg) contrast (Fig. 2*C* and *D*). HWHH increases are also seen using CRF stimuli for the cells shown in the second (45%; Fig. 2*E* and *F*), third (55%; Fig. 2*I* and *J*) and fourth (63%; Fig. 2*M* and *N*) columns. Additional example cells are shown in Fig. 3*G–N*, including two cells that show more than a 150% increase in tuning width for CRF-confined stimulation; one increasing 24.3 deg, from 16.0 deg (Fig. 3*H*, top) to 40.3 deg (Fig. 3*H*, bottom), and another that increases more than 30 deg, from 19.9 deg (Fig. 3*J*, top) to 50.1 deg (Fig. 3*J*, bottom). By comparison, changes in tuning width for CRF + ECS stimulation is relatively small (−6%, −4%, −16% and 34%, respectively, between rows 3 and 4 across the four columns in Fig. 2; see also Fig. 3*K–N*).

Results from the example cells are supported by the population data as well (Fig. 3*A–F*). For a majority of the 130 neurons tested with the CRF-confined stimulus there is an increase in tuning width at high contrast as indicated by the rightward shift in the scatter plot shown in Fig. 3*A* and the positive percentage change values shown in the histogram in Fig. 3*E*. Moreover, comparison of the means for low and high contrasts reveal a statistically significant ($P < 0.0001$) 40% increase in HWHH for the population, from 23.7 ± 0.8 deg at low contrast to 33.0 ± 1.1 deg at high contrast (Fig. 3*C*, left). On the other hand, inclusion of the ECS in a largely overlapping neuronal population ($n = 107$) does not result in a statistically significant change in mean HWHH (24.1 ± 1.0 deg at low contrast;

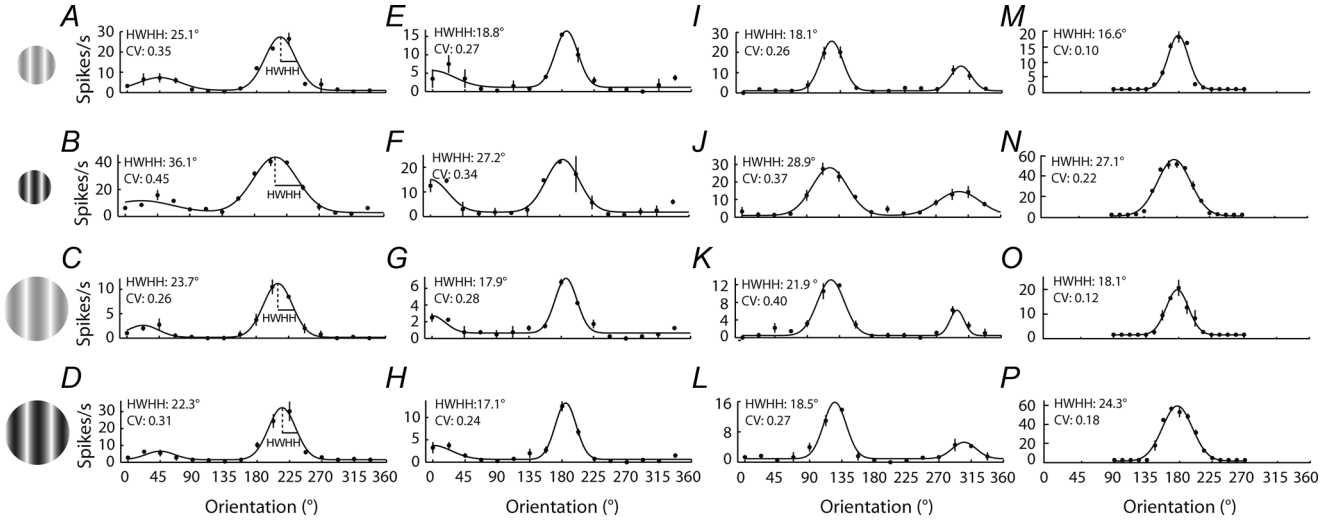

Figure 2. Orientation tuning of representative V1 neurons varies with contrast depending on stimulus size
Orientation tuning curves are shown for four example neurons, two complex cells (*A–D* and *E–H*) and two simple cells (*I–L* and *M–P*), in response to four stimulus conditions: low contrast CRF (*A*, *E*, *I* and *M*; row 1), high contrast CRF (*B*, *F*, *J* and *N*; row 2), low contrast CRF + ECS (*C*, *G*, *K* and *O*; row 3), and high contrast CRF + ECS (*D*, *H*, *L* and *P*; row 4). For these example cells, tuning width broadens when contrast is increased for the CRF condition (row 1 to row 2), but remains similar, invariant, when contrast is increased for the CRF + ECS condition (row 3 to row 4). Tuning width is measured as the half-width at half-height (HWHH) as indicated in the left column, and corresponding values are given in each panel. Circular variance (CV) values are also provided.

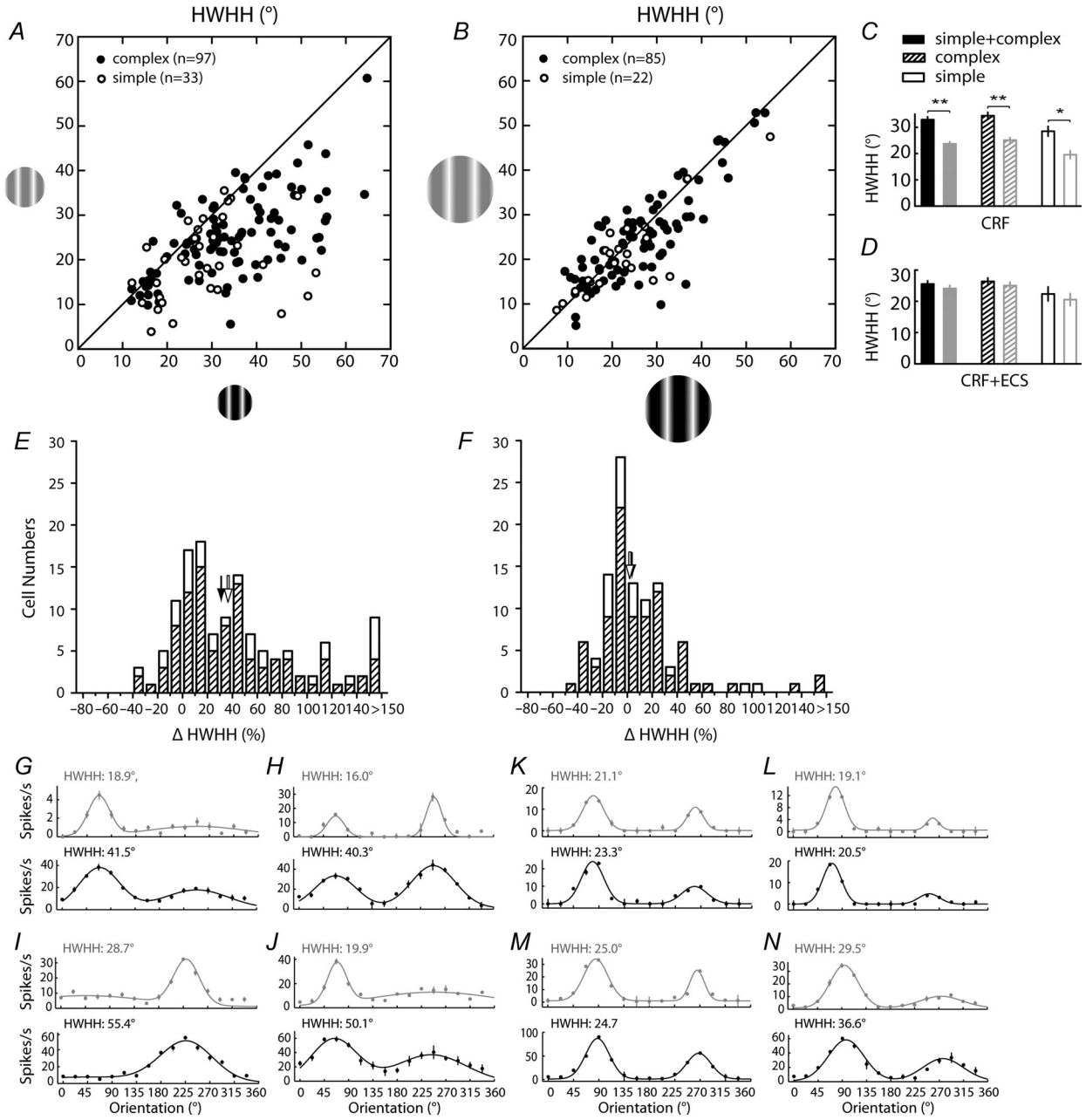

Figure 3. Orientation tuning width for the V1 cell population broadens when contrast is increased for CRF stimuli, but is invariant to contrast when the ECS is included

Scatter plots show the relationship between the HWHH at low (*y*-axis) and high (*x*-axis) contrast for the CRF (*A*) and CRF + ECS (*B*) conditions. The 105 neurons shown in *B* are a subset of the 130 neurons shown in *A*. Complex and simple cells are shown as black and white filled circles, respectively. To facilitate comparisons, resulting means from the scatter plots are presented in the bar graphs in *C* and *D*; black bars represent high contrast, grey bars represent low contrast. Error bars show the standard error of the mean. Single and double asterisks indicate significance at $P = 0.001$ and $P < 0.0001$, respectively. For all cell types (filled bars), and for complex (hatched bars) and simple (open bars) cells independently, the HWHH increases significantly when contrast is increased from low to high for the CRF (*C*), but does not change significantly for the CRF + ECS (*D*). Histograms in *E* and *F* show the percentage change in HWHH at high and low contrasts for the populations of cells shown in *A* and *B*. Hatched and open bars represent complex and simple cell counts, respectively. Positive percentage change values indicate that HWHH is broader at high compared to low contrast, whereas negative values indicate the HWHH is narrower at high contrast. Black and white arrows indicate the medians for complex and simple cells, respectively. Orientation tuning curves are shown for eight example neurons, four (*G–J*) corresponding to the CRF conditions plotted in *A*, and four (*K–N*) corresponding to the CRF + ECS conditions plotted in *B*; grey traces (top) represent low contrast and black traces (bottom) represent high contrast.

25.5 ± 1.0 deg at high contrast; $P = 0.29$; Fig. 3*D*, left), with a tighter distribution of cells found around the unity line in the scatter plot shown in Fig. 3*B*.

These results show that the average orientation tuning of V1 cells varies with contrast when using optimal CRF-confined stimulation, but is contrast invariant when the ECS is also included. Stimuli confined to the CRF are considered to activate mainly the feed-forward and local cortical inputs, whereas the inclusion of the ECS is thought to recruit longer-range cortical circuits such as horizontal projections from within V1 and feedback from higher visual areas which are characterized by a much larger spatial extent of their receptive fields (Angelucci *et al.* 2002; Cavanaugh *et al.* 2002*b*; Xing *et al.* 2005; Cantone *et al.* 2005; Angelucci & Sainsbury, 2006; Hashemi-Nezhad & Lyon, 2012; Liu *et al.* 2014). To better determine a link between the CRF mediated contrast variance and feed-forward pathways, we further subdivided our neuron population into simple and complex cells, with the idea that simple cells in cat are generally considered the main recipient of feed-forward geniculate afferents due to their higher concentration in the geniculate input layers 4 and 6 (Hubel & Wiesel, 1962; Gilbert, 1977), and should therefore show as much, if not more, contrast variance to CRF stimulation than complex cells. Accordingly, we find statistically significant contrast variance to orientation tuning for the populations of both cell types (Fig. 3*A*, *C* and *E*). Moreover, the magnitude of the change in tuning width is greater for simple cells ($n = 33$), with the population average HWHH increasing 45% from 19.6 ± 1.5 deg at low contrast to 28.5 ± 1.9 deg at high contrast ($P = 0.001$; Fig. 3*C*, right), compared to 37% for complex cells ($n = 97$; 25.1 ± 0.9 deg at low contrast; 34.4 ± 1.3 deg at high contrast; $P < 0.0001$; Fig. 3*C*, middle). It should be noted that the sharper orientation tuning of simple cells observed here is consistent with previous reports in cat (Henry *et al.* 1974; Rose & Blakemore, 1974; Leventhal & Hirsch, 1978; Schummers *et al.* 2007), ferret (Alitto & Usrey, 2004) and macaque monkey (De Valois *et al.* 1982; Ringach *et al.* 2002).

While CRF-confined stimuli lead to contrast variance, what is it about adding the ECS that leads to contrast invariance? For 135 V1 neurons we compared the tuning widths obtained using the CRF and the CRF + ECS at high contrast (Fig. 4*A*) and find that the addition of the ECS significantly narrows the orientation tuning width for the population by an average of 24% (CRF: 32.1 ± 1.0 deg; CRF + ECS: 24.5 ± 0.9 deg; $P < 0.0001$; Fig. 4*C*, left). This effect is exemplified by comparing rows 2 and 4 for the neurons shown in Fig. 2.

Sharpening of orientation tuning due to stimulus expansion beyond the CRF has been reported previously for V1 neurons in cat (Henry *et al.* 1974; Chen *et al.* 2005) and macaque monkey (Xing *et al.* 2005), and has been linked to a subtractive suppression induced by the ECS (Okamoto *et al.* 2009). However, such comparisons have only been made with high contrast. Here we find that with low contrast, in 105 of the 135 neurons tested above, tuning width is unchanged ($P = 0.43$; Fig. 4*B* and *D*). Comparing rows 1 and 3 of our example neurons in Fig. 2, it is apparent that the ECS at low contrast leads to suppression, just as it does under high contrast (rows 2 and 4 in Fig. 2). Yet, tuning width is not significantly affected for the cell population under low contrast conditions. Therefore, the net effect of surround suppression at high and low contrast is to bring the two HWHH values within range leading to the observed contrast invariance.

One issue to address is that for the 130 neurons examined for the CRF condition (Fig. 3*A*) the average CRF size at low contrast (9.6 ± 3.8 deg) was significantly larger than the high contrast CRF size (8.0 ± 3.6 deg; $P < 0.001$; see example in Fig. 1*B*). This larger CRF size for low contrast is consistent with previous reports of V1 neurons in macaque monkey (Sceniak *et al.* 1999; Cavanaugh *et al.* 2002*b*; Tailby *et al.* 2007) and cat (Hashemi-Nezhad & Lyon, 2012). Relative to the large size of the ECS seen for both contrasts (24 deg), the increase in CRF size from high to low contrast is small. While it may be possible that low contrast CRF expansion could have led to the sharper tuning, giving rise to our finding of contrast variance of orientation tuning under CRF conditions, we feel that this is not the case. This is because low contrast CRF expansion serves to facilitate responses rather than suppress (see Fig. 1*B*; Sceniak *et al.* 1999; Cavanaugh *et al.* 2002*b*; Hashemi-Nezhad & Lyon, 2012) and should not have the same sharpening effect on tuning as seen for the larger suppressive ECS at high contrast. Accordingly, we compared the change in CRF size to the change in HWHH and found little correlation ($r = 0.05$; Fig. 5). Furthermore, the CRF size was either the same at both contrasts ($n = 40$), larger at high contrast ($n = 10$), or included control conditions where the high and low contrast CRF sizes were matched ($n = 25$; see below for more details). Under all of these conditions the low contrast CRF size is the same ($n = 65$) or smaller ($n = 10$) than the high contrast CRF size, and there is still a statistically significant 32% increase in tuning width from low (24.8 ± 1.1 deg) to high (32.7 ± 1.4 deg) contrast ($P < 0.0001$; Fig. 6). Therefore, the difference in CRF size at low and high contrast for some neurons does not account for the observed population contrast variance of orientation tuning.

Analysed in more detail, for the subgroup of 50 cells where the CRF size at high and low contrast is the same (circles in Fig. 6) or larger at high contrast ('+' symbols in Fig. 6), there is a 30% average increase in tuning width that is likewise highly significant ($P < 0.001$). For the 17 cells where high contrast size is increased to match the size of the CRF at low contrast (squares in Fig. 6), there is a 40% average increase in HWHH at high contrast that is also statistically significant ($P = 0.035$). For the cells where

low contrast size was reduced to match the size of the high contrast CRF ($n = 8$; triangles in Fig. 6), the average HWHH at high contrast is 23% wider than at low contrast, but this effect is not statistically significant ($P = 0.33$) probably due, at least in part, to the small number of cells. It should be noted that this condition, where the low contrast stimulus was smaller than the preferred low contrast CRF size, often yielded unreliable responses and resulted in fewer examples from this control being collected.

Another potential confound is the possibility of systematic variability due to contrast in the quality of Gaussian fits used to determine the HWHH. For example, reduced responsivity at low contrast leads to lower signal to noise that could result in poorer fits that may skew the tuning widths. To address this, we calculated the goodness of fit (R^2) for each condition using eqn (2) and plotted the change in R^2 against the change in HWHH between low and high contrast for the CRF (Fig. 7*A*) and CRF + ECS (Fig. 7*B*) conditions, for the same cells plotted in Fig. 3*A* and *B*. As seen in Fig. 7*A*, large changes in HWHH for the CRF-confined stimulus occur regardless of the level of change (negative or positive, large or small) in fit quality. Overall, for the CRF and CRF + ECS conditions, the distribution of R^2 change is largely confined to within ± 0.10, and the trend lines indicate only a weak positive correlation with HWHH change for CRF ($r = 0.08$; Fig. 7*A*) and CRF + ECS ($r = 0.12$; Fig. 7*B*) stimuli.

Finally, while several previous studies report contrast invariance of HWHH for V1 neurons, one study by Alitto & Usrey (2004) found that a more global measure

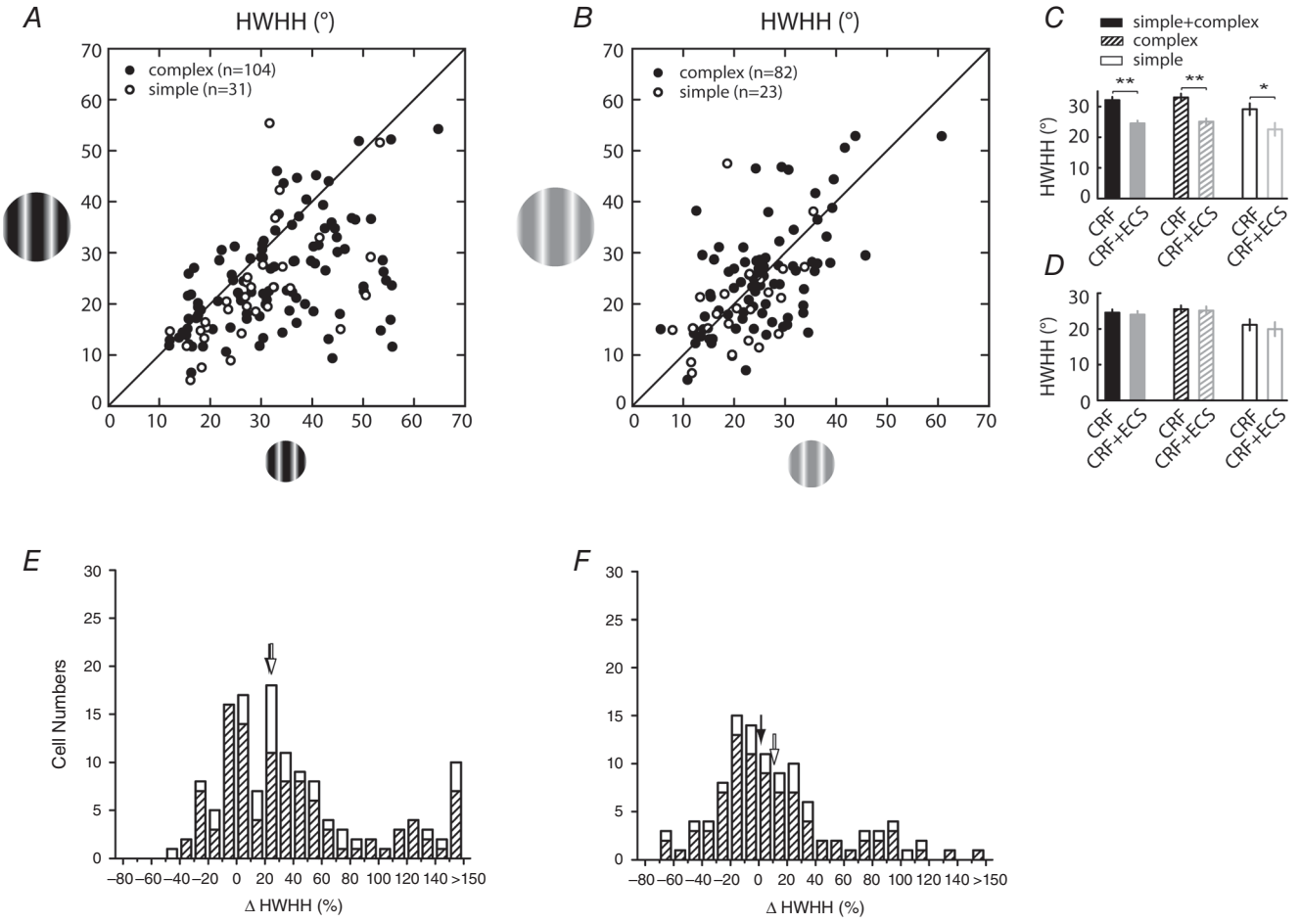

Figure 4. Contrast-invariant orientation tuning can be attributed to the inclusion of the ECS at high contrast
Scatter plots show the relationship between the HWHH for the CRF (*x*-axis) and CRF + ECS (*y*-axis) stimuli at high (*A*) and low (*B*) contrast. The 105 neurons shown in *B* are a subset of the 135 neurons shown in *A*. To facilitate comparisons, resulting means from the scatter plots are presented in the bar graphs in *C* and *D*. Histograms in *E* and *F* show the percentage change in HWHH at high and low contrasts for the populations of cells shown in *A* and *B*. Other conventions are the same as in Fig. 3. Single and double asterisks indicate significance at $P = 0.009$ and $P < 0.0001$, respectively. The addition of the ECS leads to a highly significant decrease in HWHH for high contrast stimuli; whereas at low contrast there is no net change in HWHH for the population.

of orientation tuning, circular variance (CV), does vary with contrast. Specifically, using large-field stimuli (H. J. Alitto, personal communication) they found that CV is reduced in ferret V1 cells when contrast is increased, or, put another way, orientation selectivity increases with increasing contrast. This result was supported by a study in macaque monkey V1 using a similar measure of orientation selectivity that only compared the orthogonal and preferred responses (O/P), where an increase in orientation selectivity followed an increase in contrast (Johnson *et al.* 2008). At first glance, that a contrast increase would yield lower CV appears to contradict our finding that higher contrasts lead to broader orientation tuning. However, CV calculations are different from those for HWHH (compare eqns (1) and (3)) with the former factoring in responses from all orientations, while the latter is mainly affected by orientations nearer to the preferred. Because of this, changes in the baseline firing rate can have a profound impact on CV, but little impact on HWHH, and resulting values from the two measures do not always correlate (Ringach *et al.* 2002). Nevertheless, to allow for comparisons with this previous work we also calculated CV (eqn (3); see examples of CV values in Fig. 2). For the CRF, the average population CV significantly increases when contrast is increased from low (0.46 ± 0.02) to high (0.50 ± 0.02; $P < 0.001$; data not shown), consistent with our observed increase in HWHH for the same neurons shown in Fig. 3*A* and *E* ($n = 130$). Conversely, for the CRF + ECS condition ($n = 107$), which can be considered similar to the large field stimuli used in Alitto & Usrey (2004), the CV is instead significantly lower at high contrast (0.45 ± 0.02) compared to low contrast (0.51 ± 0.02; $P < 0.02$; data not shown). Therefore, our results for large-field stimuli are consistent with Alitto & Usrey (2004); increasing the contrast of large-field stimuli reduces CV, yet HWHH is invariant (see Fig. 3*B*).

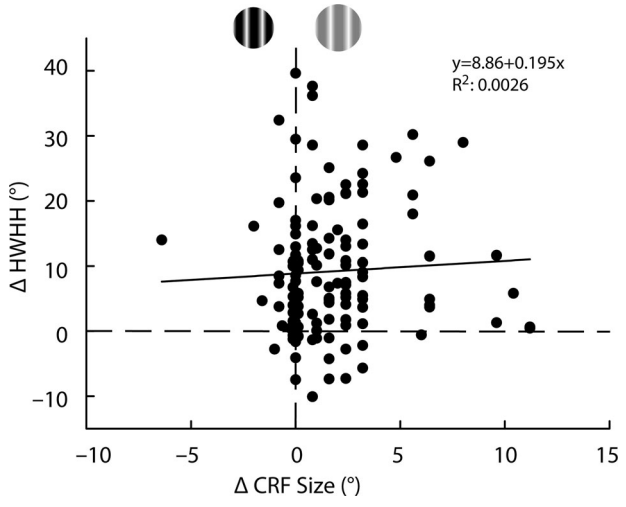

Figure 5. Change in CRF size does not account for contrast variance
For the 130 cells in Fig. 3*A* we plotted change in CRF size between high and low contrast conditions (*x*-axis) against change in HWHH (*y*-axis). For 40 cells there was no change in CRF size due to contrast (plotted along the vertical dashed line). An additional 10 cells had CRF sizes at high contrast that were larger than at low contrast (negative values on the *x*-axis). The remaining 80 neurons showed an increase in CRF size at low contrast (positive values on the *x*-axis). Overall, increase in HWHH at high contrast (positive values on the *y*-axis) occurs regardless of change in CRF size ($R^2 = 0.0026$), resulting in little correlation ($r = 0.05$) as indicated by the trend line.

Discussion

In the present study we find that the phenomenon of contrast-invariant orientation tuning in cat V1 neurons depends on the involvement of the extraclassical surround (ECS). Conversely, we demonstrate that when only the

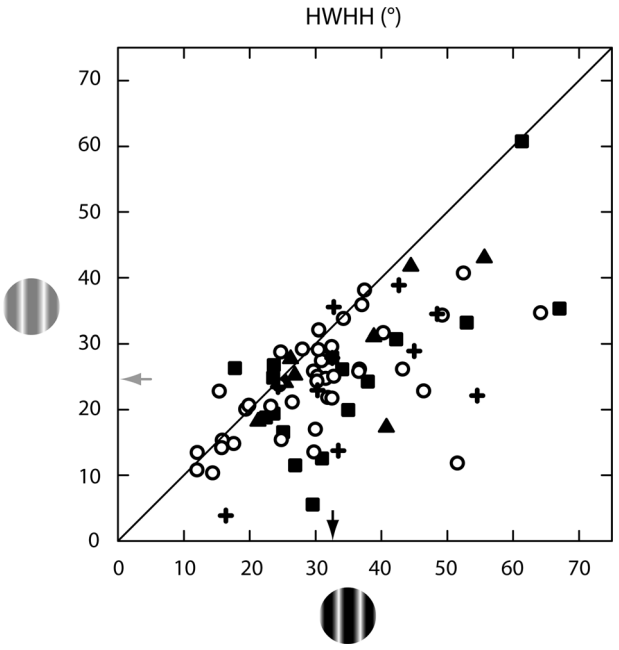

Figure 6. Contrast variance of orientation tuning remains when controlling for low contrast CRF expansion
The scatter plot shows the relationship between HWHH at low (*y*-axis) and high (*x*-axis) contrast for the CRF condition in a subset of 75 of the 130 neurons shown in Fig. 3*A*. For 50 neurons, the values are the same as given in Fig. 3*A* which include 40 cells where the CRF sizes are the same at both contrasts (circles), and 10 cells where the CRF is larger at high than at low contrast (+ symbols). For the remaining 25 neurons, HWHH values were recalculated for one of the two contrast conditions where either the high contrast size was increased to match that of the low contrast CRF size ($n = 17$; squares) or the low contrast size was reduced to match that of the high contrast CRF size ($n = 8$; triangles). Under these stimulus conditions the average low contrast size is equivalent to ($n = 65$) or smaller than ($n = 10$) the average high contrast size, and there is a highly statistically significant change in mean HWHH (indicated by arrows) between the two contrasts (24.8 ± 1.1 deg at low contrast; 32.7 ± 1.4 deg at high contrast; $P < 0.0001$).

smaller classical receptive field (CRF) of V1 neurons is stimulated, orientation tuning width is contrast variant.

Recurring evidence of contrast-invariant orientation tuning in V1 (Sclar & Freeman, 1982; Skottun *et al.* 1987; Anderson *et al.* 2000; Alitto & Usrey, 2004) has been used to challenge the classic Hubel and Wiesel (Hubel & Wiesel, 1962) explanation, that converging excitatory feed-forward afferents from the lateral geniculate nucleus (LGN) lead to the emergence of orientation tuning because it predicted broader tuning widths at higher contrasts (Rose & Blakemore, 1974; Troyer *et al.* 1998; Carandini, 2007). However, we find here that when stimuli are optimized for the CRF, orientation tuning is no longer contrast invariant for the V1 population, but is significantly broader at high contrast. That contrast variance occurs for the CRF, but not for larger stimuli, is somewhat in line with the original feed-forward proposal since an argument can be made that the CRF is more optimal at isolating the impact of geniculo-cortical inputs (Angelucci *et al.* 2002; Cavanaugh *et al.* 2002*b*; Xing *et al.* 2005; Angelucci & Sainsbury, 2006).

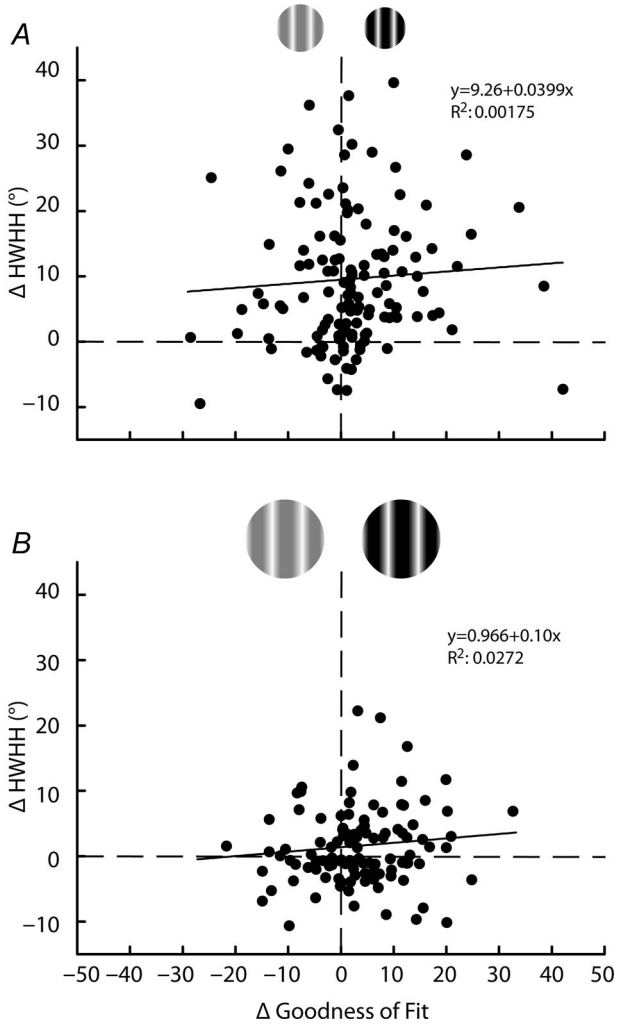

Figure 7. Contrast variance of orientation tuning does not strongly correlate with variation in goodness of fit
Change in HWHH between high and low contrast (*y*-axis) for the CRF (*A*) and CRF + ECS (*B*) conditions are plotted against the change in the goodness of fit ($R^2 \times 100$) for high and low contrast (*x*-axis). Positive values on the *x*-axis indicate better fits at high contrast; positive values on the *y*-axis indicate broader tuning width at high contrast. Dashed lines indicate zero change for each axis. Change in the goodness of fit accounts for very little of the contrast variance ($R^2 = 0.00175$ in *A*; $R^2 = 0.0272$ in *B*). Trend lines are also provided and indicate little correlation (see Results).

In support of feed-forward connections underpinning the contrast variance a study by Nowak & Barone (2009) demonstrated that the orientation tuning bandwidth of marmoset monkey V1 neurons broadened when contrast was increased for briefly flashed large-field stimuli, but was invariant to stimuli shown for several seconds. Despite using large-field stimuli, which undoubtedly included the ECS, the brief flash and early neural response is likely to emphasize and reflect feed-forward mechanisms, whereas prolonged exposure is more likely to reflect cortical mechanisms that are slower to emerge based on the temporal dynamics of V1 neuron responses (Xing *et al.* 2005; Alitto & Usrey, 2008; Liu *et al.* 2013*b*).

At the same time, our results showing that the ECS contributes to invariance suggests that explanations of the phenomenon need to incorporate long-range cortical mechanisms which could lead to recruitment of broadly tuned local inhibition (e.g. Somers *et al.* 2002). This is because the main contribution to the ECS is likely through long-range cortical connections linking across a wider representation of the visual field rather than feed-forward inputs which are more restricted in their extent of receptive field space (Angelucci *et al.* 2002; Cantone *et al.* 2005; Angelucci & Sainsbury, 2006; Hashemi-Nezhad & Lyon, 2012). These long-range connections, which are primarily from excitatory pyramidal neurons, can target local inhibitory neurons (Ahmed *et al.* 1994; Anderson *et al.* 1994; Anderson & Martin, 2009; Liu *et al.* 2013*a*) leading to di-synaptic suppression (Hirsch & Gilbert, 1991; Weliky *et al.* 1995). While long-range cortical circuits arise from two distinct sources – horizontal connections from within V1 and feedback from higher visual areas (see Angelucci *et al.* 2002; Bardy *et al.* 2009; Nassi *et al.* 2013; Liu *et al.* 2014) – a number of studies suggest that the feedback, rather than intrinsic horizontal connections, is more likely to contribute to suppression that is broadly tuned to orientation (see Stettler *et al.* 2002; Hashemi-Nezhad & Lyon, 2012; Liu *et al.* 2013*a*,*b*). Consistent with a role for feedback, inactivation of higher visual areas has been shown to lead to a broadening of orientation tuning in cat V1 (Wang *et al.* 2000, 2007). However, in such instances broadening was accompanied by a reduction in response magnitude which suggests involvement of some mechanisms other than those explained by the 'iceberg effect'. On the other hand, results in macaque monkey

from Nassi *et al.* (2013), specifically report that a reduction in V1 response magnitude from feedback inactivation only happens when the stimulus size is confined to the CRF. For larger stimuli, which include the ECS, inactivation of feedback instead results in facilitation of V1 responses. Differences in results reported by these two groups could be a product of different higher visual areas inactivated or possible species differences. Di-synaptic horizontal connections within V1 are another possibility because such circuits can cover a large extent of receptive field similar to feedback from higher visual areas (Liu *et al.* 2014) and existing evidence reveals that a greater proportion of horizontal intrinsic inputs synapse directly onto inhibitory neurons compared to feedback from higher visual areas suggesting a more direct role in the reduction of response amplitude (Anderson & Martin, 2009; Liu *et al.* 2013*a*).

Prior to V1, extraclassical surround suppression is already present in the retina and LGN and is also broadly tuned to orientation (Nolt *et al.* 2004; Sceniak *et al.* 2006; Alitto & Usrey, 2008). Moreover, one study has even demonstrated that orientation-tuned neurons in the LGN show contrast invariance that may be partially mediated through local inhibitory neurons (Naito *et al.* 2013). However, we expect that any feed-forward effects on contrast invariance to orientation tuning would be limited since the ECS covered in LGN accounts for a relatively small component of the full receptive field extent of the suppressive surround (Angelucci & Sainsbury, 2006). Other alternatives to cortically mediated suppression such as synaptic noise or trial-to-trial variability in the membrane potential are affected by changes in contrast and have been implicated in contrast invariance of orientation tuning as well (Finn *et al.* 2007; Palmer & Miller, 2007). Whether such mechanisms are modulated by the presence of the ECS is unclear as stimulus size has not been systematically evaluated. In addition, results by Sadagopan & Ferster (2012) using electrically evoked cortical suppression suggest that cortical activity may not play a role in trial-to-trial variability for lower (4–32%) contrast stimuli, leaving open the possibility that portions of the ECS which are carried through feed-forward pathways (Sceniak *et al.* 2006; Alitto & Usrey, 2008) may be involved.

Despite contrast invariance of orientation tuning having long been considered by many to result through a suppressive mechanism, mediated through cortical inhibition or otherwise, size of the visual stimulus has not previously been considered in studies examining the phenomenon. Yet, it is now established that extending the stimulus size beyond the classical receptive field typically has a suppressive effect on V1 neuron responses (DeAngelis *et al.* 1994; Sengpiel *et al.* 1997; Walker *et al.* 2000; Akasaki *et al.* 2002; Cavanaugh *et al.* 2002*b*; Liu *et al.* 2011) and leads to a significant sharpening in the orientation tuning width (Henry *et al.* 1974; Chen *et al.* 2005; Xing *et al.* 2005; Okamoto *et al.* 2009), at least for high contrast. Therefore, our findings of contrast invariance for the ECS and contrast variance for the CRF should not be entirely unexpected.

As noted above, several previous studies used only large-field stimuli, similar to our CRF + ECS (Skottun *et al.* 1987; Anderson *et al.* 2000; Alitto & Usrey, 2004). The first study to demonstrate contrast invariance used 10 deg stimuli (Sclar & Freeman, 1982), which may better approximate the CRF, though it is 25% larger than the average CRF size for our population. However, one study did use stimuli of optimal size (Finn *et al.* 2007) similar to our CRF condition. This study examined simple cells recorded by whole cell patch clamp and found, in contrast to our results, that several exhibited contrast-invariant orientation tuning. Conversely, an additional subset of neurons recorded extracellularly showed significant broadening of HWHH to increasing contrast (see their Supplemental Fig. 3), more in line with our results (Fig. 3*E*). Whether the difference in recording procedures played a role in this discrepancy is unclear, and other factors such as which cortical layers the simple cells were sampled from could also play a role.

Conclusion

We find that the phenomenon of contrast invariance of orientation tuning of V1 neurons is a product of co-stimulation of the CRF and ECS. Because a majority of a V1 neuron's ECS is mediated through long-range cortical circuits, such as feedback from higher visual areas (Angelucci *et al.* 2002) and/or di-synaptic horizontal connections within V1 (Gilbert & Wiesel, 1989; Liu *et al.* 2014), as opposed to feed-forward LGN projections (Angelucci & Sainsbury, 2006), it seems more likely that contrast invariance is a product of longer-range cortical circuits rather than solely an emergent feature of feed-forward inputs. Conversely, showing that when stimulus sizes are optimized to isolate feed-forward inputs as much as possible by using the CRF, the prediction of Hubel and Wiesel's (1962) original feed-forward model on the emergence of orientation tuning regains some of the plausibility previously lost. This is not to say that feed-forward circuits have no role in contrast invariance, or that cortical mechanisms are not also at play when only using the CRF stimulus (Xing *et al.* 2011), but that they are not enough to result in complete contrast invariance of orientation tuning. These results serve as a reminder that stimulus size can have a significant impact on a cell's response and should be considered carefully when addressing mechanisms of feature selectivity in V1 neurons.

References

Ahmed B, Anderson JC, Douglas RJ, Martin KA & Nelson JC (1994). Polyneuronal innervation of spiny stellate neurons in cat visual cortex. *J Comp Neurol* **341**, 39–49.

Akasaki T, Sato H, Yoshimura Y, Ozeki H & Shimegi S (2002). Suppressive effects of receptive field surround on neuronal activity in the cat primary visual cortex. *Neurosci Res* **43**, 207–220.

Alitto HJ & Dan Y (2010). Function of inhibition in visual cortical processing. *Curr Opin Neurobiol* **20**, 340–346.

Alitto HJ & Usrey WM (2004). Influence of contrast on orientation and temporal frequency tuning in ferret primary visual cortex. *J Neurophysiol* **91**, 2797–2808.

Alitto HJ & Usrey WM (2008). Origin and dynamics of extraclassical suppression in the lateral geniculate nucleus of the macaque monkey. *Neuron* **57**, 135–146.

Anderson JC, Douglas RJ, Martin KA & Nelson JC (1994). Synaptic output of physiologically identified spiny stellate neurons in cat visual cortex. *J Comp Neurol* **341**, 16–24.

Anderson JC & Martin AC (2009). The synaptic connections between cortical areas V1 and V2 in macaque monkey. *J Neurosci* **29**, 11283–11293.

Anderson JS, Lampl I, Gillespie DC & Ferster D (2000). The contribution of noise to contrast invariance of orientation tuning in cat visual cortex. *Science* **290**, 1968–1972.

Angelucci A, Levitt JB, Walton EJ, Hupe JM, Bullier J & Lund JS (2002). Circuits for local and global signal integration in primary visual cortex. *J Neurosci* **22**, 8633–8646.

Angelucci A & Sainsbury K (2006). Contribution of feedforward thalamic afferents and corticogeniculate feedback to the spatial summation area of macaque V1 and LGN. *J Comp Neurol* **498**, 330–351.

Bardy C, Huang JY, Wang C, Fitzgibbon T & Dreher B (2009). 'Top-down' influences of ipsilateral or contralateral postero-temporal visual cortices on the extra-classical receptive fields of neurons in cat's striate cortex. *Neuroscience* **158**, 951–968.

Cantone G, Xiao J, McFarlane N & Levitt JB (2005). Feedback connections to ferret striate cortex: direct evidence for visuotopic convergence of feedback inputs. *J Comp Neurol* **487**, 312–331.

Carandini M (2007). Melting the iceberg: contrast invariance in visual cortex. *Neuron* **54**, 11–13.

Carandini M & Ferster D (2000). Membrane potential and firing rate in cat primary visual cortex. *J Neurosci* **20**, 470–484.

Carandini M & Heeger DJ (1994). Summation and division by neurons in primate visual cortex. *Science* **264**, 1333–1336.

Cavanaugh JR, Bair W & Movshon JA (2002*a*). Nature and interaction of signals from the receptive field center and surround in macaque V1 neurons. *J Neurophysiol* **88**, 2530–2546.

Cavanaugh JR, Bair W & Movshon JA (2002*b*). Selectivity and spatial distribution of signals from the receptive field surround in macaque V1 neurons. *J Neurophysiol* **88**, 2547–2556.

Chen G, Dan Y & Li CY (2005). Stimulation of non-classical receptive field enhances orientation selectivity in the cat. *J Physiol* **564**, 233–243.

DeAngelis GC, Freeman RD & Ohzawa I (1994). Length and width tuning of neurons in the cat's primary visual cortex. *J Neurophysiol* **71**, 347–374.

De Valois RL, Yund EW & Hepler N (1982). The orientation and direction selectivity of cells in macaque visual cortex. *Vision Res* **22**, 531–544.

Ferster D (1988). Spatially opponent excitation and inhibition in simple cells of the cat visual cortex. *J Neurosci* **8**, 1172–1180.

Ferster D & Miller KD (2000). Neural mechanisms of orientation selectivity in the visual cortex. *Annu Rev Neurosci* **23**, 441–471.

Finn IM, Priebe NJ & Ferster D (2007). The emergence of contrast-invariant orientation tuning in simple cells of cat visual cortex. *Neuron* **54**, 137–152.

Freeman TC, Durand S, Kiper DC & Carandini M (2002). Suppression without inhibition in visual cortex. *Neuron* **35**, 759–771.

Gilbert CD (1977). Laminar differences in receptive field properties of cells in cat primary visual cortex. *J Physiol* **268**, 391–421.

Gilbert CD & Wiesel TN (1989). Columnar specificity of intrinsic horizontal and corticocortical connections in cat visual cortex. *J Neurosci* **9**, 2432–2442.

Hashemi-Nezhad M & Lyon DC (2012). Orientation tuning of the suppressive extraclassical surround depends on intrinsic organization of V1. *Cereb Cortex* **22**, 308–326.

Henry GH, Dreher B & Bishop P (1974). Orientation of cells in cat striate cortex. *J Neurophysiol* **37**, 1394–1409.

Hirsch JA, Alonso JM, Reid RC & Martinez LM (1998). Synaptic integration in striate cortical simple cells. *J Neurosci* **18**, 9517–9528.

Hirsch JA & Gilbert CD (1991). Synaptic physiology of horizontal connections in the cat's visual cortex. *J Neurosci* **11**, 1800–1809.

Hubel DH & Wiesel TN (1962). Receptive fields, binocular interaction and functional architecture in the cat's visual cortex. *J Physiol* **160**, 106–154.

Johnson EN, Hawken MJ & Shapley R (2008). The orientation selectivity of color-responsive neurons in macaque V1. *J Neurosci* **28**, 8096–8106.

Leventhal AG & Hirsch HV (1978). Receptive-field properties of neurons in different laminae of visual cortex of the cat. *J Neurophysiol* **41**, 948–962.

Liu Y, Arreola M, Coleman C & Lyon DC (2014). Very long-range disynaptic V1 connections through layer 6 pyramidal neurons revealed by transneuronal tracing with rabies virus. *Eye Brain* **6**, 45–56.

Liu YJ, Ehrengruber MU, Negwer M, Shao HJ, Cetin AH & Lyon DC (2013*a*). Tracing inputs to inhibitory or excitatory neurons of mouse and cat visual cortex with a targeted rabies virus. *Curr Biol* **23**, 1746–1755.

Liu YJ, Hashemi-Nezhad M & Lyon DC (2011). Dynamics of extraclassical surround modulation in three types of V1 neurons. *J Neurophysiol* **105**, 1306–1317.

Liu YJ, Hashemi-Nezhad M & Lyon DC (2013*b*). Sharper orientation tuning of the extraclassical suppressive-surround due to a neuron's location in the V1 orientation map emerges late in time. *Neuroscience* **229**, 100–117.

Naito T, Okamoto M, Sadakane O, Shimegi S, Osaki H, Hara S, Kimura A, Ishikawa A, Suematsu N & Sato H (2013). Effects of stimulus spatial frequency, size, and luminance contrast on orientation tuning of neurons in the dorsal lateral geniculate nucleus of cat. *Neurosci Res* **77**, 143–154.

Nassi JJ, Lomber SG & Born RT (2013). Corticocortical feedback contributes to surround suppression in V1 of the alert primate. *J Neurosci* **33**, 8504–8517.

Nolt MJ, Kumbhani RD & Palmer LA (2004). Contrast-dependent spatial summation in the lateral geniculate nucleus and retina of the cat. *J Neurophysiol* **92**, 1708–1717.

Nowak LG & Barone P (2009). Contrast adaptation contributes to contrast-invariance of orientation tuning of primate V1 cells. *PLoS One* **4**, e4781.

Okamoto M, Naito T, Sadakane O, Osaki H & Sato H (2009). Surround suppression sharpens orientation tuning in the cat primary visual cortex. *Eur J Neurosci* **29**, 1035–1046.

Palmer SE & Miller KD (2007). Effects of inhibitory gain and conductance fluctuations in a simple model for contrast-invariant orientation tuning in cat V1. *J Neurophysiol* **98**, 63–78.

Reid RC & Alonso JM (1996). The processing and encoding of information in the visual cortex. *Curr Opin Neurobiol* **6**, 475–480.

Ringach DL, Shapley RM & Hawken MJ (2002). Orientation selectivity in macaque V1: diversity and laminar dependence. *J Neurosci* **22**, 5639–5651.

Rose D & Blakemore C (1974). An analysis of orientation selectivity in the cat's visual cortex. *Exp Brain Res* **20**, 1–17.

Sadagopan S & Ferster D (2012). Feedforward origins of response variability underlying contrast invariant orientation tuning in cat visual cortex. *Neuron* **74**, 911–923.

Sceniak MP, Chatterjee S & Callaway EM (2006). Visual spatial summation in macaque geniculocortical afferents. *J Neurophysiol* **96**, 3474–3484.

Sceniak MP, Ringach DL, Hawken MJ & Shapley R (1999). Contrast's effect on spatial summation by macaque V1 neurons. *Nat Neurosci* **2**, 733–739.

Schummers J, Cronin B, Wimmer K, Stimberg M, Martin R, Obermayer K, Koerding K & Sur M (2007) Dynamics of orientation tuning in cat V1 neurons depend on location within layers and orientation maps. *Front Neurosci* **1**, 145–159.

Sclar G & Freeman RD (1982). Orientation selectivity in the cat's striate cortex is invariant with stimulus contrast. *Exp Brain Res* **46**, 457–461.

Sengpiel F, Sen A & Blakemore C (1997). Characteristics of surround inhibition in cat area 17. *Exp Brain Res* **116**, 216–228.

Skottun BC, Bradley A, Sclar G, Ohzawa I & Freeman RD (1987). The effects of contrast on visual orientation and spatial frequency discrimination: a comparison of single cells and behavior. *J Neurophysiol* **57**, 773–786.

Skottun BC, De Valois RL, Grosof DH, Movshon JA, Albrecht DG & Bonds AB (1991). Classifying simple and complex cells on the basis of response modulation. *Vision Res* **31**, 1079–1086.

Somers D, Dragoi V & Sur M (2002). Orientation selectivity and its modulation by local and long-range connections in visual cortex. In *The Cat Primary Visual Cortex*, ed. Payne BR & Peters A, pp. 471–520. Academic Press, San Diego.

Sompolinsky H & Shapley R (1997). New perspectives on the mechanisms for orientation selectivity. *Curr Opin Neurobiol* **7**, 514–522.

Stettler DD, Das A, Bennett J & Gilbert CD (2002). Lateral connectivity and contextual interactions in macaque primary visual cortex. *Neuron* **36**, 739–750

Stimberg M, Wimmer K, Martin R, Schwabe L, Marino J, Schummers J, Lyon DC, Sur M & Obermayer K (2009). The operating regime of local computations in primary visual cortex. *Cereb Cortex* **19**, 2166–2180.

Tailby C, Solomon SG, Peirce JW & Metha AB (2007). Two expressions of 'surround suppression' in V1 that arise independent of cortical mechanisms of suppression. *Vis Neurosci* **24**, 99–109.

Tan AY, Brown BD, Scholl B, Mohanty D & Priebe NJ (2011). Orientation selectivity of synaptic input to neurons in mouse and cat primary visual cortex. *J Neurosci* **31**, 12339–12350.

Troyer TW, Krukowski AE, Priebe NJ & Miller KD (1998). Contrast-invariant orientation tuning in cat visual cortex: thalamocortical input tuning and correlation-based intracortical connectivity. *J Neurosci* **18**, 5908–5927.

Walker GA, Ohzawa I & Freeman RD (2000). Suppression outside the classical cortical receptive field. *Vis Neurosci* **17**, 369–379.

Wang C, Waleszczyk WJ, Burke W & Dreher B (2000). Modulatory influence of feedback projections from area 21a on neuronal activities in striate cortex of the cat. *Cereb Cortex* **10**, 1217–1232.

Wang C, Waleszczyk WJ, Burke W & Dreher B (2007). Feedback signals from cat's area 21a enhance orientation selectivity of area 17 neurons. *Exp Brain Res* **182**, 479–490.

Weliky M, Kandler K, Fitzpatrick D & Katz LC (1995). Patterns of excitation and inhibition evoked by horizontal connections in visual cortex share a common relationship to orientation columns. *Neuron* **15**, 541–552.

Xing D, Ringach DL, Hawken MJ & Shapley RM (2011). Untuned suppression makes a major contribution to the enhancement of orientation selectivity in macaque V1. *J Neurosci* **31**, 15972–15982.

Xing D, Shapley RM, Hawken MJ & Ringach DL (2005). Effect of stimulus size on the dynamics of orientation selectivity in macaque V1. *J Neurophysiol* **94**, 799–812.

Additional information

Competing interests

The authors declare that they do not have any conflicts of interest.

Author contributions

The experiments were performed in the laboratory of D.C.L. All authors contributed to (1) the conception and design of the experiments, (2) the collection, assembly, analysis and interpretation of the data, and (3) the writing and revising of the manuscript. All authors aproved the final version of the manuscript.

Funding

This work was partially supported by funding from the Whitehall Foundation, grant no. 2009-12-44 (D.C.L.).

Acknowledgements

We thank Heny Alitto for helpful discussions regarding stimulus parameters and data analysis.